processes

MDPI

Article

Kinetics of Reductive Dissolution of a Magnetite Specimen Using Oxalic Acid

Hye Rim Kim [1], Jae Kwan Park [1], Su In Lee [1], Wonzin Oh [2], Jeongju Kim [3], Chorong Kim [3] and Byung-Chul Lee [1,*]

[1] Department of Chemical Engineering, Hannam University, Daejeon 34054, Korea; mnb1756@naver.com (H.R.K.); qkrworhks01@gmail.com (J.K.P.); enddl_dl@naver.com (S.I.L.)
[2] Research Institute of Advanced Energy Technology, Kyungpook National University, Daegu 41566, Korea; wonzin@knu.ac.kr
[3] KHNP Central Research Institute, Daejeon 34101, Korea; jeongju.kim@khnp.co.kr (J.K.); chorong.kim@khnp.co.kr (C.K.)
* Correspondence: bclee@hnu.kr; Tel.: +82-42-629-8838

Abstract: The removal of radionuclides from the primary coolant system of nuclear power plants occurs with the dissolution of corrosion metal oxide layers deposited with the radionuclides. Kinetic dissolution experiments were conducted with a synthetic magnetite specimen in the form of a thin plate using an aqueous solution of oxalic acid as a reducing agent. The effects of acid concentration and temperature were investigated on the kinetics of the reductive dissolution of a magnetite specimen. In particular, the kinetic experiments were performed in a wide temperature range from low (57 °C) to high (120 °C), above the normal boiling point of water. The dissolution of magnetite increased with increasing acid concentration and temperature. The acid concentration dependence of the dissolution reaction rate of Fe at a given temperature was correlated with the nth power of the oxalic acid concentration. Additionally, the temperature dependence of the dissolution reaction rate of Fe at a fixed oxalic acid concentration was studied with an Arrhenius-type equation.

Keywords: magnetite specimen; chemical decontamination; reductive dissolution; kinetics; oxalic acid

check for updates

Citation: Kim, H.R.; Park, J.K.; Lee, S.I.; Oh, W.; Kim, J.; Kim, C.; Lee, B.-C. Kinetics of Reductive Dissolution of a Magnetite Specimen Using Oxalic Acid. *Processes* **2022**, *10*, 696. https://doi.org/10.3390/pr10040696

Academic Editor: Gade Pandu Rangaiah

Received: 1 March 2022
Accepted: 2 April 2022
Published: 3 April 2022

Publisher's Note: MDPI stays neutral with regard to jurisdictional claims in published maps and institutional affiliations.

Copyright: © 2022 by the authors. Licensee MDPI, Basel, Switzerland. This article is an open access article distributed under the terms and conditions of the Creative Commons Attribution (CC BY) license (https://creativecommons.org/licenses/by/4.0/).

1. Introduction

Radioactive materials generated from a nuclear power plant (NPP) reactor are deposited in the form of corrosion oxide layers on the surface of the coolant system, thereby increasing the level of radiation. Accordingly, it is necessary to reduce the radiation level by removing the corrosion oxide layers through decontamination before the decommissioning operation. According to the NPP decommissioning plan, the Kori Unit 1, one of the pressurized water reactors in Korea, is expected to perform chemical decontamination of the reactor coolant system after permanent shutdown [1]. Chemical decontamination is a key technology that can remove more than 95% of the radionuclide inventory from the primary coolant system of NPPs. Recently, extensive research on the current status and prospects for various decontamination technologies in NPPs has been conducted [2]. In general, the corrosion oxide layers deposited on the inner surface of structures of the coolant system are composed of metal oxides of iron, nickel, and chromium. The removal of the radionuclides from the primary coolant system occurs with the dissolution of corrosion metal oxide layers deposited with the radionuclides.

Chemical decontamination through the oxidative and reductive dissolution of the metal oxides has so far been recognized as the most effective method. In a number of experimental results and practical reports, organic acids such as oxalic acid [1,3–8], citric acid [9–11], ethylelenediamine tetraacetic acid [11], and mixtures thereof were used

as strong reducing reagents due to their faster dissolution rates and chelating capacities. Additionally, reductive dissolution through the addition of reducing reagents like hydrazine [12,13] has been reported with effective experimental results.

The decontamination processes using oxalic acid have been most widely developed to reductively dissolve the magnetite oxide film, which constitutes most of the corrosion oxides in the NPP cooling system. The mechanisms and kinetics related to the magnetite dissolution in the oxalic acid solution have been extensively studied. Salmimies et al. [6] measured the solubility of magnetite in oxalic acid by using samples of synthetic magnetite powder and natural magnetite powder while varying temperature and oxalic acid concentration. The solubility was highly dependent on the oxalic acid concentration and the dependence on temperature was small. The solubility of natural magnetite in oxalic acid showed somewhat more complex behavior due to particle size distribution and impurities. Thermodynamic and kinetic dissolution experiments were performed at different temperatures and different oxalic and sulfuric acid ratios using synthetic magnetite powder [7]. Increasing the oxalic acid content in the solution phase yielded higher solubilities as well as accelerated kinetics.

The objective of the present experimental study is to investigate the effects of reaction temperature and acid concentration on the kinetics of the reductive dissolution of magnetite. The dissolution experiments were conducted with a synthetic magnetite specimen in the form of a thin plate, using the aqueous oxalic acid solution at different concentrations and temperatures. Until now, there have been many studies on the reductive dissolution of magnetite using oxalic acid, but most studies have used powder as the magnetite materials. When using a magnetite powder sample, it is difficult to accurately measure the reductive dissolution rate, because the surface area decreases irregularly due to the dissolution of powder consisting of various sizes and shapes. On the other hand, the magnetite sample used in this study is a specimen made by sintering magnetite powder at a high temperature. This can be considered a novel approach. The crystal structure and surface properties of our magnetite specimen samples remained unchanged during the dissolution experiments. In addition, it should be emphasized that most of the decontamination experiments performed so far were conducted at temperatures below 100 °C, but our experiments were also conducted at higher temperatures (120 °C).

2. Experimental

2.1. Materials and Analytical Methods

In order to observe the characteristics of the reductive decontamination reaction of corrosion oxides, a magnetite specimen (Fe_3O_4) was used as the test material, and oxalic acid was used as the reducing agent. The dimensions and a surface image of the thin plate magnetite specimen are shown in Figure 1. The magnetite specimen used in our work was purchased from the Kojundo Chemical Laboratory Co., LTD (Saitama, Japan). The certificate of analysis for the magnetite specimen sample was provided by the company and is given in Table 1. Solid oxalic acid dihydrate ($H_2C_2O_4 \cdot 2H_2O$: CAS no. 6153-56-6) with a purity of 99.5% (EP grade) from Daejung Chemicals and Metals (Sinan, Korea) was used to formulate (prepare) the leaching solutions. Deionized water was used to prepare the solution and analyze the samples in all the experiments.

For the magnetite specimen samples, the surface morphology and elemental compositions of the materials were measured using a field emission scanning electron microscope (FE-SEM) (Jeol model JSM-7610F Plus) equipped with energy dispersive x-ray spectroscopy (EDS). The area scan method was used for the EDS analysis. An inductively coupled plasma mass spectrometer (ICP-MS) (Perkin Elmer model NexION 2000) was used to analyze the concentration of Fe^{2+} ions dissolved into the aqueous solution from the magnetite specimen during the reductive decontamination. It had a detection limit of less than 1.5 $ng \cdot L^{-1}$ (ppt) for ^{56}Fe.

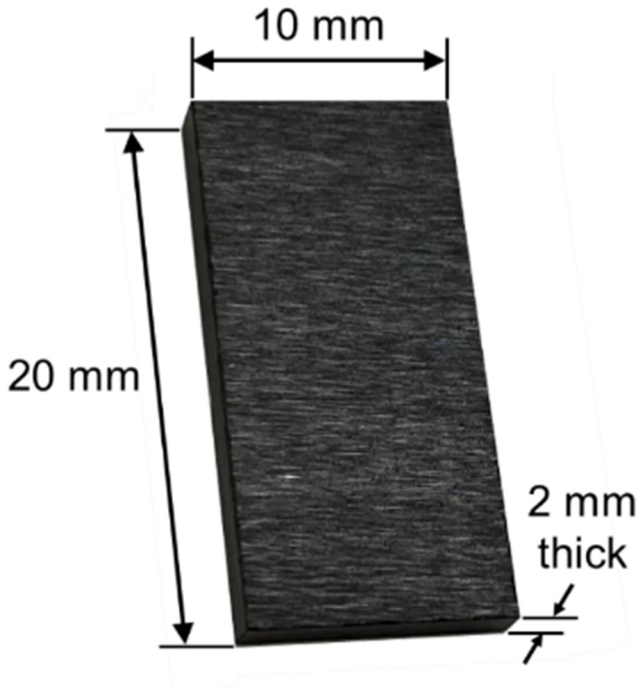


Figure 1. Shape and dimensions of the magnetite specimen used in this work.

Table 1. Certificate * of elemental analysis for the magnetite (Fe_3O_4) specimen sample.

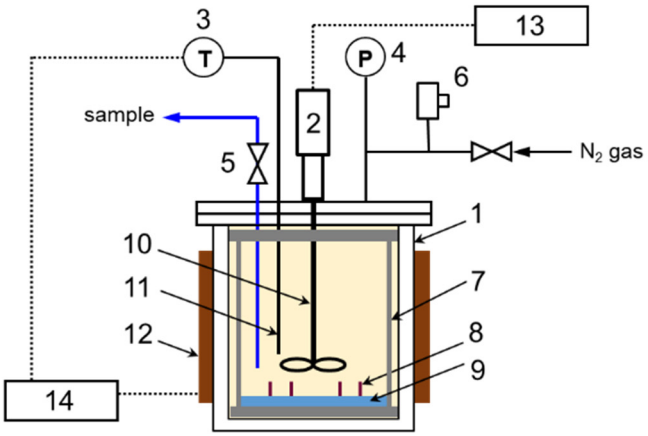
Purity		99.8%
Metal impurities	Element	Amount [%]
	Al	0.02
	Cr	0.01
	Mn	0.02
	Na	0.02
	Ni	0.005
	Si	0.02
	Total	0.095

* Provided by the Kojundo Chemical Laboratory Co.

2.2. Apparatus and Procedure

Figure 2 shows a schematic diagram of the experimental apparatus for dissolving Fe_3O_4 from the magnetite specimen using an aqueous oxalic acid solution as a reducing agent. The leaching experiments were carried out in a stainless steel reactor equipped with a thermostat to maintain constant temperature in the reacting mixture. The heart of the system is the high-temperature and high-pressure cylindrical reactor, which has the following dimensions: 70 mm internal diameter, 150 mm height, and an internal working volume of about 580 mL. A magnetic drive with an agitator was installed to mix the solution inside the reactor. Two pitched paddle agitators with four paddles, which had diameters of 37 mm and 50 mm, were mounted on the agitator shaft to for better agitation. The distance between the agitator and the specimen holder placed on the bottom of the reactor is about 5 mm. No baffles are installed on the inner wall of the reactor; however, it is believed that the thin plate-shaped magnetite specimen mounted in the specimen holder can partially play the role as a baffle during stirring. A ceramic band heater is attached to the outer wall of the reactor to heat the solution in the reactor. Inside the wall of the reactor, a thermocouple, an agitator and shaft, and a sampling line in the reactor are all Teflon-coated to prevent corrosion of materials by the oxalic acid solution. In order to prevent the aqueous solution in the reactor from boiling or evaporating, the upper part

of the reactor was connected to a nitrogen gas cylinder in which the pressure was kept constant at 1.5 bar. Figure 3 shows a photograph of the holder made of Teflon material to fix the magnetite specimen inside the reactor.



1. Main vessel
2. Magnetic stirrer
3. Temperature indicator
4. Pressure gauge
5. Sampling valve and line
6. Safety valve
7. Specimen holder basket
8. Specimen inserted
9. Specimen holder
10. Agitator
11. Thermocouple
12. Band heater
13. RPM meter
14. Temperature controller

Figure 2. A schematic diagram of the experimental apparatus for high-temperature reductive decontamination.

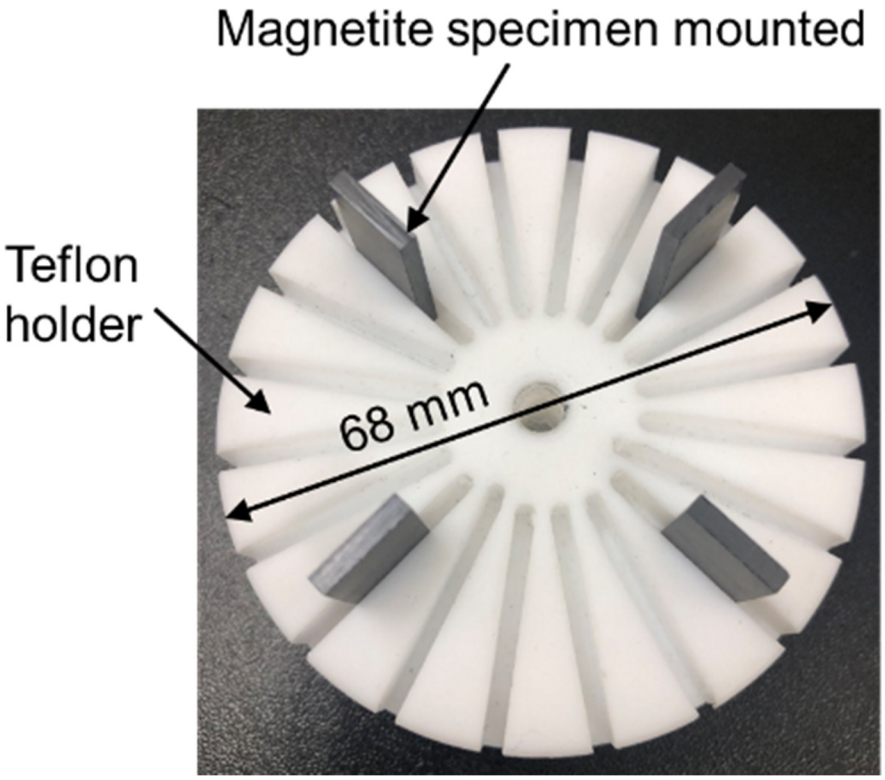


Figure 3. Photograph of the specimen holder.

The experimental conditions are presented in Table 2. Oxalic acid concentration and reaction temperature were determined in consideration of the NPP's chemical decontam-

ination application range. The experimental procedure is as follows: First, the amounts of oxalic acid, magnetite specimen, and deionized water corresponding to certain experimental conditions were quantified using precision balances (AND models HM-300 and GX-1003A) measuring ± 0.1 mg and ± 1 mg, respectively. After inserting the magnetite specimen into the holder, the holder was placed inside the reactor. The prepared oxalic acid aqueous solution was introduced into the reactor, and then the flange at the top of the reactor was coupled. The reaction temperature was set by operating the band heater, and the dissolution reaction was conducted while stirring the reaction solution. The stirring speed was 300 rpm.

Table 2. Experimental conditions for the reductive dissolution of magnetite specimen using oxalic acid.

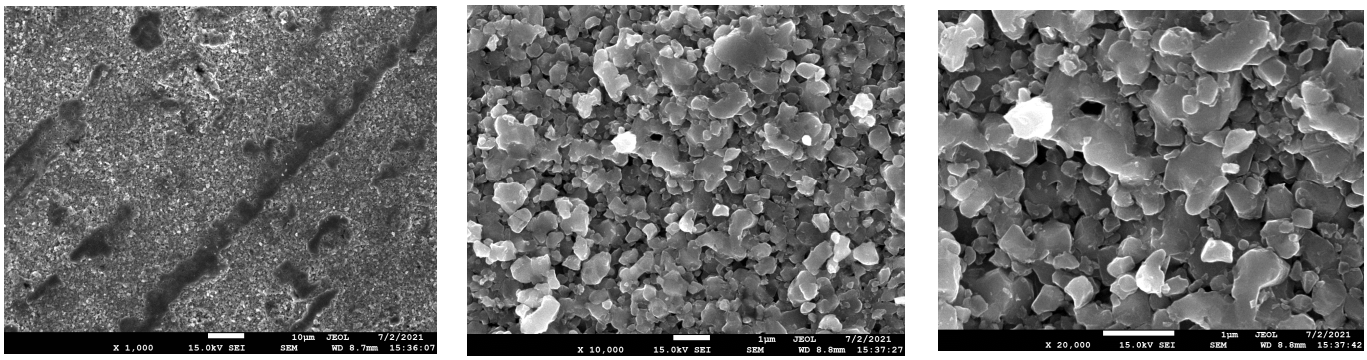
Operating Variable	Experimental Condition
Reaction temperature, T_{rxn} [°C]	57, 82, 95, 105, 120
Concentration of oxalic acid, C_{OA} [mmol·L^{-1}]	10, 15, 20, 30, 40
Reaction time, t [min]	180 max.
Reactor pressure, P [bar]	1.5~1.9 (under N_2 gas)
Volume of reaction solution, V [mL]	500
Number of magnetite specimen used in experiments	1

During the dissolution reaction, samples were taken from the reaction solution at different time intervals. A glass vial was used to take the sample from the reactor, after which the sample was diluted with DI water ten times to avoid any precipitation caused by changes in the temperature. A total reaction time of 120 min or 180 min was employed to obtain the kinetic data for the dissolution reaction, depending on the variable. Finally, the concentration of the dissolved Fe present in the sample solution was measured through the ICP-MS analysis.

3. Results and Discussion

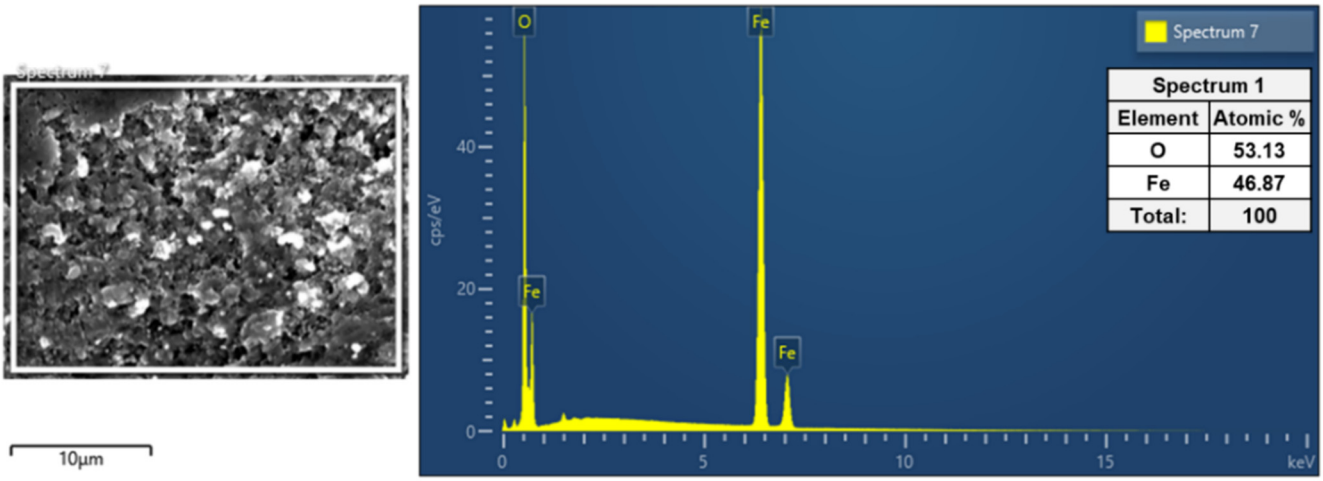
Figure 4 shows the FE-SEM images and the EDS analysis result for the magnetite specimen sample used in this work. It is revealed that the specimen consists of 68.77 atomic % Fe and 29.25 atomic % O. The FE-SEM images of the magnetite specimen sample after the dissolution reaction are given in Figure 5. Note that the images shown in Figures 4 and 5 are compared at the same magnifications. Compared to the SEM images of the specimen before the dissolution reaction shown in Figure 4, it seems that the surface of the magnetite specimen was slightly roughened due to the reductive dissolution by the oxalic acid solution. In particular, this is well shown in the × 1000 magnification image.

A kinetic study of the reductive dissolution of the magnetite specimen in oxalic acid medium was performed with the experimental conditions shown in Table 2. The key experimental parameters were reaction temperature and oxalic acid concentration. Five different temperatures were chosen to observe the effect of temperature on the kinetics of the dissolution of the magnetite specimen. The concentrations for oxalic acid were 10, 15, 20, 30, and 40 mmol·L^{-1}. During the dissolution reaction, small amounts of samples (about 5 mL) were collected from the aqueous solution of oxalic acid at preset reaction times, and the leached Fe content in the aqueous solution (based on concentration) was analyzed for each sample.



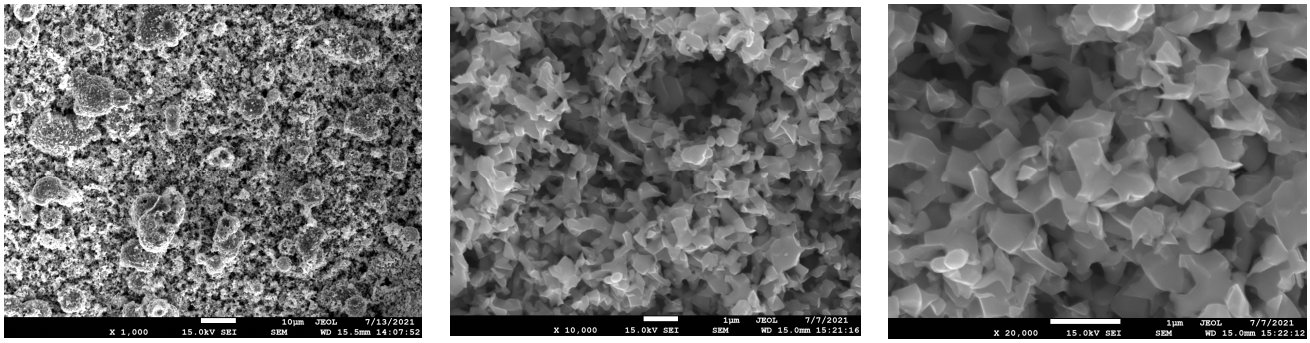
×1000 ×10,000 ×20,000

(**a**) FE-SEM images



(**b**) Result of EDS analysis

Figure 4. FE-SEM images of the raw sample of magnetite specimen before reductive dissolution test.



×1000 ×10,000 ×20,000

Figure 5. FE-SEM images of the magnetite specimen sample after reductive dissolution test.

3.1. Effect of Oxalic Acid Concentration

The effect of oxalic acid concentration on the concentration of the Fe^{2+} ions leached from the magnetite specimen was studied. The oxalic acid concentration varied at 10, 15, 20, 30, and 40 mmol·L^{-1} and the reaction temperature was kept constant. The experimental results are shown in Table 3. The effect of acid concentration on the dissolution of magnetite was clearly seen with oxalic acid. Noticeable differences in kinetics were observed when using oxalic acid with concentrations of 10 to 40 mmol·L^{-1}. Increased

oxalic acid concentration yielded increased dissolution of Fe from the magnetite specimen. Therefore, it can be seen that the reductive reaction occurred more rapidly as the oxalic acid concentration increased. The solution temperature and the reaction time are also listed in Table 3. It took approximately 50 min for the solution temperature to reach close to the set temperature. The actual average value of the solution temperature maintained after the solution temperature reached the set temperature was approximately 94 °C.

Table 3. Experimental kinetic data of reductive dissolution of magnetite specimen using oxalic acid at different acid concentrations (C_{OA}) at a constant temperature around 94 °C.

Reaction Time, t [min]	T_{soln} [a] **[°C]**	$C_{Fe^{2+}}$ [b] **[mmol·L^{-1}]**	T_{soln} **[°C]**	$C_{Fe^{2+}}$ **[mmol·L^{-1}]**	T_{soln} **[°C]**	$C_{Fe^{2+}}$ **[mmol·L^{-1}]**
	C_{OA} = 10 mmol·L^{-1} (T_{rxn} [c] = 94 °C)		C_{OA} = 15 mmol·L^{-1} (T_{rxn} = 94 °C)		C_{OA} = 20 mmol·L^{-1} (T_{rxn} = 94 °C)	
0	18	0	18	0	17	0
20	50	0.036	51	0.053	49	0.045
40	83	0.201	83	0.275	83	0.336
50	89 [d]	0.383 [d]	93 [d]	0.530 [d]	91 [d]	0.654 [d]
60	94 [d]	0.535 [d]	96 [d]	0.741 [d]	95 [d]	0.954 [d]
90	96 [d]	0.928 [d]	93 [d]	1.335 [d]	94 [d]	1.909 [d]
120	97 [d]	1.403 [d]	95 [d]	2.072 [d]	97 [d]	2.834 [d]
	C_{OA} = 30 mmol·L^{-1} (T_{rxn} = 94 °C)		C_{OA} = 40 mmol·L^{-1} (T_{rxn} = 95 °C)			
0	17	0	20	0		
20	50	0.049	57	0.104		
40	84	0.479	88	0.701		
50	91 [d]	0.955 [d]	93 [d]	1.430 [d]		
60	95 [d]	1.430 [d]	96 [d]	2.072 [d]		
90	94 [d]	2.622 [d]	93 [d]	3.537 [d]		
120	96 [d]	3.876 [d]	96 [d]	5.365 [d]		

[a] Real-time temperature of aqueous solution in the reactor. [b] Concentration of Fe^{2+} ions leached from the magnetite specimen. [c] Average reaction temperature. [d] Data used for obtaining the average reaction temperature (T_{rxn}) and for performing the linear fitting of the dissolution reaction rate of Fe ($r(x) = dC_{Fe^{2+}}/dt$).

From the reaction time when the reaction temperature almost reached the set temperature, the concentration of dissolved Fe^{2+} increased almost linearly with time. Only the data showing such linear increases were taken and presented in Figure 6. The linear plots were also given together with the data. For the five oxalic acid concentrations examined, the dissolution reaction rates of Fe were calculated from the slopes of the linear fits shown in Figure 6, and the results are listed in Table 4. In all cases, the R^2 values were greater than 0.99, meaning that the fits were almost perfectly linear. In Table 4, in addition to the absolute concentration itself, the relative concentration denoted by x was used to express the concentration of oxalic acid used in the dissolution reaction. x is defined as the ratio of the actual oxalic acid concentration (C_{OA}) to the reference oxalic acid concentration ($C_{OA,R}$), which is expressed in a dimensionless form as: $x = C_{OA}/C_{OA,R}$. In this work, $C_{OA,R}$ was arbitrarily set to 20 mmol·L^{-1}. Note that the acid concentration of 20 mmol·L^{-1} was the same concentration adopted when studying the effect of temperature on the dissolution of magnetite (see Table 5).

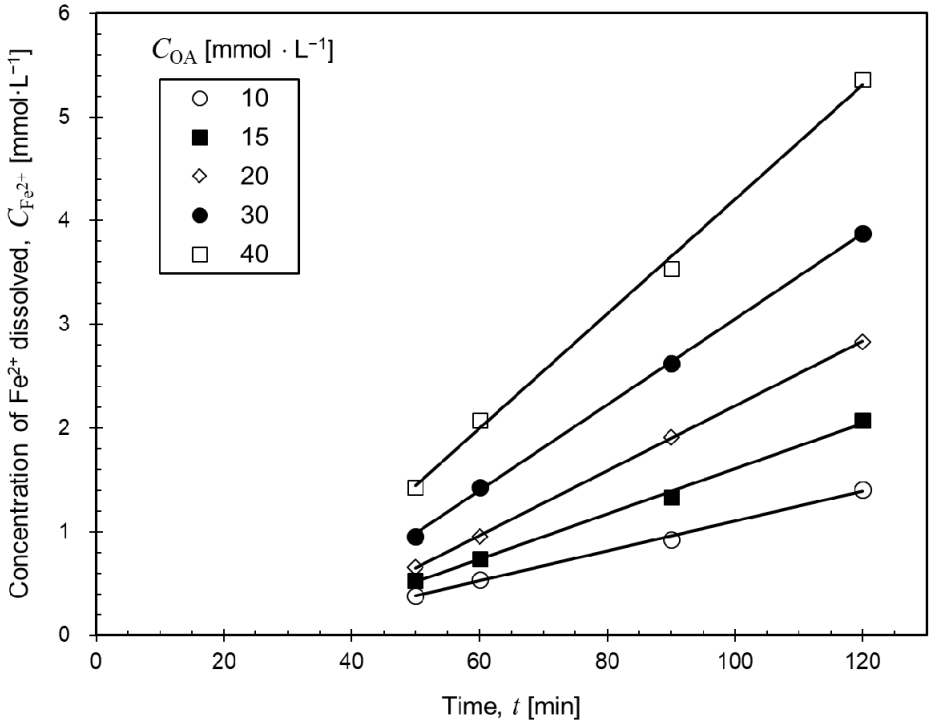


Figure 6. Linear plots of the concentration of Fe^{2+} ion dissolved with respect to reaction time at different oxalic acid concentrations.

Table 4. Results of the linear fit of dissolution reaction rates of Fe at different oxalic acid concentrations.

C_{OA} [mmol·L^{-1}]	$x = \frac{C_{OA}}{C_{OA,R}}$ *	Dissolution Reaction Rate of Fe, $r(x)(=\frac{dC_{Fe^{2+}}}{dt})$ [mmol·L^{-1}·min^{-1}]	R^2
10	0.5	0.014	0.998
15	0.75	0.022	0.997
20	1	0.031	0.999
30	1.5	0.041	0.999
40	2	0.055	0.998

* Reference oxalic acid concentration: $C_{OA,R} = 20$ mmol·L^{-1}.

Figure 7 shows the effect of oxalic acid concentration on the dissolution rate of magnetite specimens at an average reaction temperature of 94 °C. The dissolution rate of Fe increased almost linearly as the oxalic acid concentration increased. The data were fitted to a power equation, and the results are presented in Figure 7. A slope from the straight line of the graph gave a reaction order of $n = 0.958$ with a coefficient of determination of $R^2 = 0.992$. Thus, the dependence of the oxalic acid concentration of the dissolution reaction rate $[r(x)]$ of the magnetite specimen at 94 °C can be expressed by the following equation:

$$r(x)|_{T=94°C} = \left.\frac{dC_{Fe^{2+}}}{dt}\right|_{T=94°C} = 0.029x^{0.958} \quad (1)$$

This indicates that the order of the dissolution reaction rate is close to 1 with respect to the oxalic acid concentration.

Table 5. Experimental kinetic data of reductive dissolution of magnetite specimen using oxalic acid at different reaction temperatures (T_{rxn}) with C_{OA} = 20 mmol·L^{-1} fixed.

Reaction Time, *t* [min]	T_{soln} [a] **[°C]**	$C_{Fe^{2+}}$ [b] **[mmol·L^{-1}]**	T_{soln} **[°C]**	$C_{Fe^{2+}}$ **[mmol·L^{-1}]**	T_{soln} **[°C]**	$C_{Fe^{2+}}$ **[mmol·L^{-1}]**
	T_{rxn}[c] = 57 °C		T_{rxn}= 82 °C		T_{rxn}= 95 °C	
0	16	0	21	0	22	0
20	37	0.118	48	0.184	54	0.114
40	55 [d]	0.164 [d]	77	0.347	85	0.513
50	58 [d]	0.330 [d]	82 [d]	0.595 [d]	91	0.884
60	59 [d]	0.489 [d]	83 [d]	0.868 [d]	94 [d]	1.287 [d]
90	55 [d]	0.814 [d]	81 [d]	1.443 [d]	94 [d]	2.099 [d]
120	59 [d]	1.229 [d]	79 [d]	2.165 [d]	96 [d]	3.221 [d]
150	56 [d]	1.583 [d]	82 [d]	2.790 [d]	97 [d]	4.022 [d]
180	58 [d]	1.776 [d]	82 [d]	3.367 [d]	96 [d]	4.384 [d]
	T_{rxn}= 105 °C		T_{rxn}= 120 °C			
0	16	0	17	0		
20	50	0.125	56	0.114		
40	87	0.451	96	0.467		
50	99	0.924	109	0.849		
60	105 [d]	1.334 [d]	116 [d]	1.318 [d]		
90	103 [d]	2.404 [d]	121 [d]	2.531 [d]		
120	106 [d]	3.449 [d]	120 [d]	3.728 [d]		
150	106 [d]	4.432 [d]	121 [d]	4.647 [d]		
180	106 [d]	5.181 [d]	120 [d]	5.608 [d]		

[a] Real-time temperature of aqueous solution in the reactor. [b] Concentration of Fe^{2+} ions leached from the magnetite specimen. [c] Average reaction temperature. [d] Data used for obtaining the average reaction temperature (T_{rxn}) and for performing the linear fitting of the dissolution reaction rate of Fe ($r(T) = dC_{Fe^{2+}}/dt$).

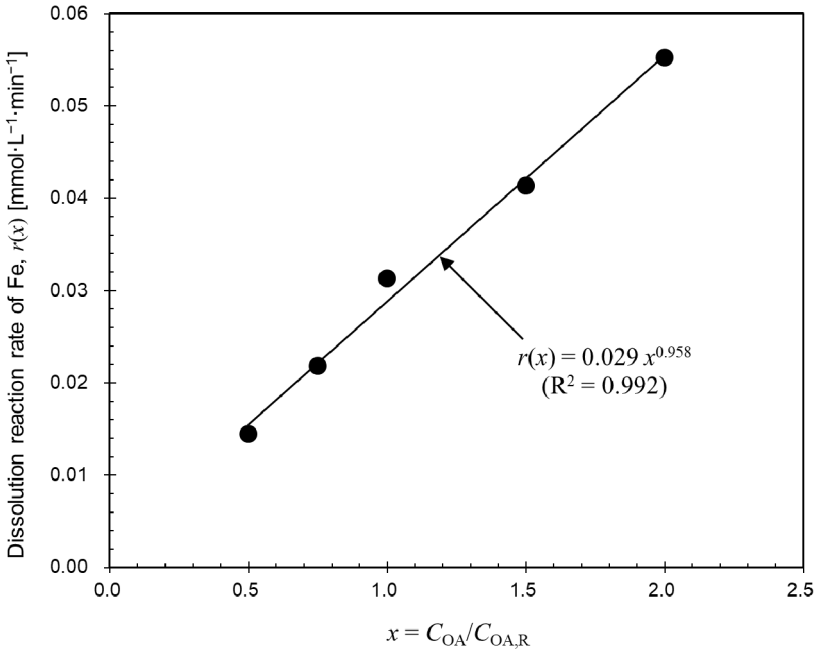


Figure 7. Dissolution reaction rate of Fe ($r(x)$) vs. oxalic acid concentration (x) at a fixed reaction temperature of 94 °C.

3.2. Effect of Reaction Temperature

Table 5 shows the experimental data for the reductive dissolution of the magnetite specimen at five different reaction temperatures. The table shows the change in the concen-

tration of the Fe^{2+} ions leached from the magnetite specimen with respect to the reaction time. Note that the concentration of oxalic acid in the aqueous solution was kept constant at 20 mmol·L^{-1}. The temperature of the solution in the reactor, according to the lapse of the reaction time, is also listed in each table. It took approximately 60 min (however, 40 min for 57 °C and 50 min for 82 °C) until the temperature of the reactor reached the set temperature. Therefore, the average value of the solution temperature after the time the solution temperature reached close to the set temperature was regarded as the reaction temperature.

As the reaction time elapsed, the concentration of the dissolved Fe^{2+} ions showed a tendency to increase. Additionally, the dissolution reaction rate of Fe^{2+} increased with the increase in the reaction temperature. Typical dissolution rate curves with a strong temperature dependence were found. Therefore, it can be seen that the reductive dissolution occurs better at high temperature than at low temperature. That means that the dissolution of Fe^{2+} using oxalic acid could be thermally activated to improve its efficiency. In particular, at the reaction time when the temperature of the reaction solution nearly reached the set temperature, the concentration of dissolved Fe^{2+} increased almost linearly with time. In order to show this trend more clearly, only the data from the time section showing the linear change were separately taken and shown in Figure 8, and the linear fits were also given together with the data.

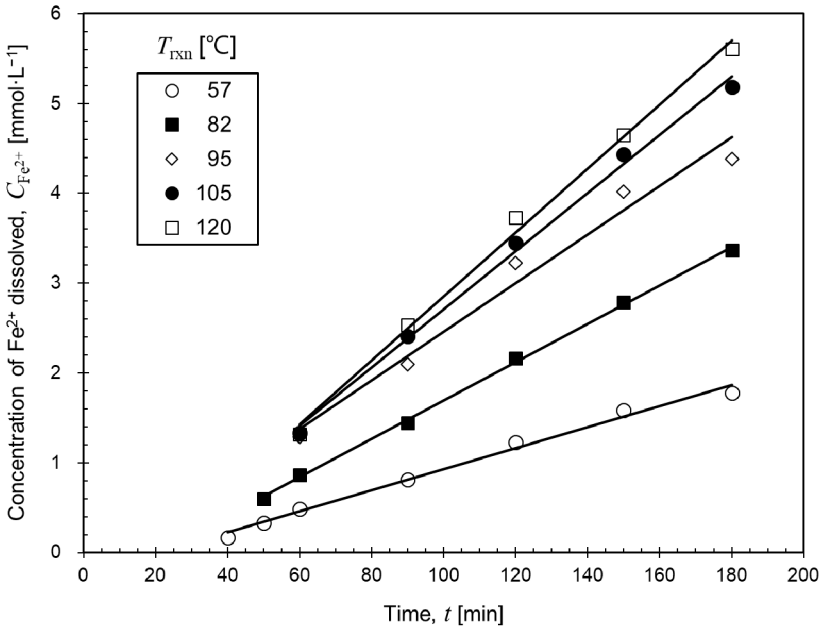


Figure 8. Linear plots of the concentration of Fe^{2+} ion dissolved with respect to reaction time at different reaction temperatures.

For each temperature tested, the dissolution reaction rate of Fe ($r(T)$) was obtained from the slope of the linear plot in Figure 8, and the results are listed in Table 6. The graphs in Figure 8 revealed straight lines for all reaction temperatures, and the coefficients of determination (R^2) of the linear fits, which expressed the goodness of the fits, were greater than 0.97. The temperature dependency of the dissolution reaction rate, $r(T)$, can be expressed in a form of the Arrhenius equation:

$$r(T) = \frac{dC_{Fe^{2+}}}{dt} = k_0 \exp\left(-\frac{E_a}{RT}\right) \quad (2)$$

where $C_{Fe^{2+}}$ is the concentration of Fe^{2+} dissolved, E_a is an apparent activation energy for the dissolution reaction, k_0 is a reaction rate constant in the Arrhenius equation, and R is the gas constant (8.314 × 10^{-3} kJ·mol^{-1}·K^{-1}).

Table 6. Results for the linear plots of the dissolution reaction rates of Fe at different reaction temperatures.

Reaction Temperature, T_{rxn} **[°C]**	**Dissolution Reaction Rate of Fe,** $r(T)(=\frac{dC_{Fe^{2+}}}{dt})$ **[mmol·L^{-1}·min^{-1}]**	R^2
57	0.012	0.991
82	0.021	0.999
95	0.027	0.975
105	0.032	0.996
120	0.036	0.996

With the aim of making the Arrhenius plot represent the variation of $\ln r(T)$ vs. $1/T$ in the range of temperatures tested in this work, the calculations shown in Table 7 were performed from the data in Table 6. Figure 9 shows the result of the Arrhenius plot representing the temperature dependence of the rate of dissolution reaction for our system. The E_a and k_0 values were obtained from the slope and intercept of the straight line of $\ln r(T)$ vs. $1/T$ in Figure 9, respectively, and are given in Table 7. Consequently, the temperature dependence of the dissolution reaction rate of Fe at $x = 1$ (C_{OA} = 20 mmol·L^{-1}) is expressed as follows:

$$r(T)|_{x=1} = 16.318 \exp\left(-\frac{19.726}{RT}\right) \quad (3)$$

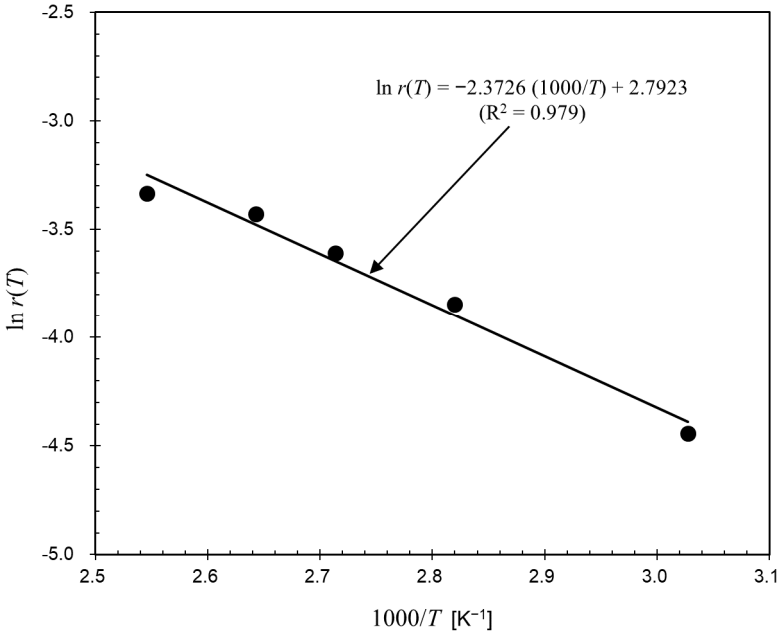


Figure 9. Arrhenius plot of the dissolution reaction rate in the studied temperature range.

Table 7. Data and results for the Arrhenius plot [$\ln r(T)$ vs. $1/T_{rxn}$] of the dissolution reaction rate of Fe with respect to the reaction temperature.

T_{rxn} **[°C]**	T_{rxn} **[K]**	$\frac{1000}{T_{rxn}}$**[K^{-1}]**	**ln**$r(T)$	E_a **[kJ·mol^{-1}]**	k_0 **[mmol·L^{-1}·min^{-1}]**	R^2
57	330.15	3.028	−4.443			
82	355.15	2.82	−3.846			
95	368.15	2.713	−3.610	19.726	16.318	0.979
105	378.15	2.643	−3.429			
120	393.15	2.546	−3.334			

4. Conclusions

From the experimental study on the kinetics of the reductive dissolution of the magnetite specimen in oxalic acid medium, the following conclusions were obtained depending on the temperature and acid concentration. The results showed that the temperature and acid concentration were of importance for the determination of the dissolution reaction kinetics. According to the results for the acid concentration dependence of the dissolution reaction rate at a given temperature, the order of reaction was observed to be $n = 0.958$, close to the first order. The temperature dependence of the dissolution reaction rate of Fe from the magnetite specimen followed the Arrhenius formula well. The activation energy of the dissolution reaction was found to be 19.726 kJ·mol^{-1}.

Author Contributions: Conceptualization, W.O. and B.-C.L.; methodology, H.R.K., J.K.P. and S.I.L.; validation, W.O. and B.-C.L.; writing—original draft preparation, B.-C.L.; writing—review and editing, B.-C.L.; supervision, J.K. and C.K.; project administration, J.K. and C.K.; funding acquisition, W.O., J.K. and C.K. All authors have read and agreed to the published version of the manuscript.

Funding: This research was funded by the Korea Institute of Energy Technology Evaluation and Planning (KETEP), grant number 20191510301310.

Institutional Review Board Statement: Not applicable.

Informed Consent Statement: Not applicable.

Data Availability Statement: Not applicable.

Conflicts of Interest: The authors declare no conflict of interest.

References

1. Kim, C.; Kim, H. Study on chemical decontamination process based on permanganic acid-oxalic acid to remove oxide layer deposited in primary system of nuclear power plant. *J. Nucl. Fuel Cycle Waste Technol.* **2019**, *17*, 15–28. [CrossRef]
2. Moon, J.K.; Kim, S.B.; Choi, W.K.; Choi, B.S.; Chung, D.Y.; Seo, B.K. The status and prospect of decommissioning technology development at KAERI. *J. Nucl. Fuel Cycle Waste Technol.* **2019**, *17*, 139–165. [CrossRef]
3. Lee, B.-C.; Oh, W. Temperature and concentration dependencies of chemical equilibrium for reductive dissolution of magnetite using oxalic acid. *J. Nucl. Fuel Cycle Waste Technol.* **2021**, *19*, 187–196. [CrossRef]
4. Lee, S.O.; Tran, T.; Park, Y.Y.; Kim, S.J.; Kim, M.J. Study on the kinetics of iron oxide leaching by oxalic acid. *Int. J. Miner. Process.* **2006**, *80*, 144–152. [CrossRef]
5. Lee, S.O.; Tran, T.; Jung, B.H.; Kim, S.J.; Kim, M.J. Dissolution of iron oxide using oxalic acid. *Hydrometallurgy* **2007**, *87*, 91–99. [CrossRef]
6. Salmimies, R.; Mannila, M.; Kallas, J.; Hakkinen, A. Acidic dissolution of magnetite: Experimental study on the effects of acid concentration and temperature. *Clays Clay Miner.* **2011**, *59*, 136–146. [CrossRef]
7. Salmimies, R.; Vehmaanpera, P.; Hakkinen, A. Acidic dissolution of magnetite in mixtures of oxalic acid and sulfuric acid. *Hydrometallurgy* **2016**, *163*, 91–98. [CrossRef]
8. Jung, J.Y.; Park, S.Y.; Won, H.J.; Kim, S.B.; Choi, W.K.; Moon, J.K.; Park, S.J. Crevice corrosion properties and chemical thermodynamic evaluation of the corrosion system. *J. Radioanal. Nucl. Chem.* **2015**, *306*, 377–383. [CrossRef]
9. Manjanna, J.; Venkateswaran, G.; Sherigara, B.S.; Nayak, P.V. Dissolution studies of chromium substi tuted iron oxides in reductive-complexing agent mixtures. *Hydrometallurgy* **2001**, *60*, 155–165. [CrossRef]
10. Larba, R.; Boukerche, I.; Alane, N.; Habbache, N.; Djerad, S.; Tifouti, L. Citric acid as an alternative lixiviant for zinc oxide dissolution. *Hydrometallurgy* **2013**, *134–135*, 117–123. [CrossRef]
11. Joseph, S.; Visalakshi, G.; Venkateswaran, G.; Moorthy, P.N. Dissolution of hematite in citric acid-EDTA-ascorbic acid mixtures. *J. Nucl. Sci. Technol.* **1996**, *33*, 479–485. [CrossRef]
12. Choi, W.K. *Development of Advanced Decontamination Technology for Nuclear Facilities*; KAERI Report No. 2012M2A8A5025655; KAERI: Daejeon, Korea, 2017.
13. Won, H.J.; Lee, W.S.; Jung, C.H.; Park, S.Y.; Choi, W.K.; Moon, J.K. A feasibility study on the decontamination of type 304 stainless steel by N_2H_4 base solution. *Asian J. Chem.* **2014**, *26*, 1327–1330. [CrossRef]